

Contents lists available at [ScienceDirect](#)

IATSS Research



## Human-like motion planning model for driving in signalized intersections<sup>☆</sup>

Yanlei Gu<sup>a,\*</sup>, Yoriyoshi Hashimoto<sup>b</sup>, Li-Ta Hsu<sup>a</sup>, Miho Iryo-Asano<sup>a</sup>, Shunsuke Kamijo<sup>a</sup>

<sup>a</sup> Institute of Industrial Science, The University of Tokyo, Japan

<sup>b</sup> Graduate School of Information Science and Technology, The University of Tokyo, Japan

### ARTICLE INFO

Available online xxxx

#### Keywords:

Motion planning  
Autonomous vehicle  
Signalized intersection  
Gap acceptance  
Pedestrian behavior

### ABSTRACT

Highly automated and fully autonomous vehicles are much more likely to be accepted if they react in the same way as human drivers do, especially in a hybrid traffic situation, which allows autonomous vehicles and human-driven vehicles to share the same road. This paper proposes a human-like motion planning model to represent how human drivers assess environments and operate vehicles in signalized intersections. The developed model consists of a pedestrian intention detection model, gap detection model, and vehicle control model. These three submodels are individually responsible for situation assessment, decision making, and action, and also depend on each other in the process of motion planning. In addition, these submodels are constructed and learned on the basis of human drivers' data collected from real traffic environments. To verify the effectiveness of the proposed motion planning model, we compared the proposed model with actual human driver and pedestrian data. The experimental results showed that our proposed model and actual human driver behaviors are highly similar with respect to gap acceptance in intersections.

© 2016 Production and hosting by Elsevier Ltd. on behalf of International Association of Traffic and Safety Sciences. This is an open access article under the CC BY-NC-ND license (<http://creativecommons.org/licenses/by-nc-nd/4.0/>).

## 1. Introduction

Recent developments in advanced driver assistance systems and autonomous robots seem to suggest that cars will be able to drive without human intervention in the near future. Thus, autonomous vehicles will join human drivers on the road soon. Currently, research studies on autonomous vehicles focus on their safety aspects to reduce accidents. These studies have adopted various sensors, such as LIDAR, radar, and vision, to perceive the surrounding environment and avoid collision with other vehicles and pedestrians. There is another critical issue in a hybrid traffic situation. Humans, including pedestrians and drivers, should not be affected by autonomous vehicles. In other words, the behavior of an autonomous vehicle is supposed to be similar to that of a human-driven vehicle, to avoid confusing pedestrians and other drivers in decision making. The accident reports on Google's driverless car also suggested that robot cars might actually be too cautious and careful. Google is actually working to correct this cautiousness and make its

cars drive more similarly to humans to reduce the number of accidents [1]. This paper proposes a human-like motion planning model that can control vehicles like humans do.

Vehicle motion models can be divided into three levels with an increasing degree of abstraction: physics-based motion models, maneuver-based motion models, and interaction-aware motion models [2]. The physics-based motion models explain the vehicle motion by velocity, acceleration, mass of the vehicle, road surface friction coefficient, and the laws of physics. This type of models can be used for predicting the evolution of the state of the vehicle [3,4], but is limited to short-term (less than 1 s) motion prediction [2]. The maneuver-based motion models represent vehicles as independent maneuvering entities and could provide long-term predictions of driver intentions. Campbell et al. and Amsalu et al. proposed to use the continuous vehicle dynamics to recognize the different driving maneuvers, including lane keeping, straightly passing intersections, and turning at intersections [5,6]. However, autonomous vehicles are expected to automatically decide the driving maneuvers on the basis of the awareness of the surrounding environment.

The interaction-aware motion models consider vehicles as maneuvering entities that interact with other road users and environment. Gindele et al. presented a dynamic Bayesian network (DBN) that can simultaneously estimate the behaviors of vehicles and anticipate their future trajectories. This estimation is achieved by recognizing the type of

<sup>☆</sup> Peer review under responsibility of International Association of Traffic and Safety Sciences.

\* Corresponding author.

E-mail address: [guyanlei@kmj.iis.u-tokyo.ac.jp](mailto:guyanlei@kmj.iis.u-tokyo.ac.jp) (Y. Gu).

situation derived from the local situational context [7,8]. Platho et al. proposed to decompose the complex situations into smaller and more manageable parts to recognize and understand the driving situations [9]. Hulsens et al. suggested that driving behavior is greatly influenced by four aspects: traffic rules, assessment of allowed actions, expected behaviors, and impacts of traffic participants on each other [10,11]. They introduced an ontology to model traffic situations at complex intersections and enabled reasoning about traffic rules for involved vehicles. Obviously, the influence of contextual information, such as traffic rules, road structure, and actions of other road users, should be considered in the motion planning model.

To model and represent human-like motion planning, we need to understand how the contextual information affects a driver's action. The influence can be modeled and analyzed on the basis of data collected from real traffic environments. In particular, most research studies on autonomous vehicles focus on right- or left-turning vehicles at intersections and discuss how vehicles pass the intersections in the case of sharing the road with other road users. The driving maneuver, in which a turning vehicle passes the intersection, is called gap acceptance. The basic idea of gap acceptance is to estimate the time difference between two consecutive pedestrians and vehicles [12]. Ragland et al. analyzed the distribution of accepted and rejected gaps in the left turn across path/opposite direction scenarios and proposed to characterize gap acceptance by a logistic model [13]. Zohdy also proposed to determine the critical gaps using a logit function [14]. Schroeder et al. explored factors associated with driver-yielding behavior at unsignalized pedestrian crossings and developed predictive models by using logistic regression [15]. Rather than at common intersections, Salamati et al. aimed to identify the contributing factors affecting the likelihood of a driver yielding to pedestrians at two-lane roundabouts [16]. Alhajyaseen et al. [17] and Wolfermann et al. [18] explained the stochastic speed profiles and the stochastic path models of free-flowing left- and right-turning vehicles from the aspect of intersection layout. Moreover, Alhajyaseen et al. [19,20] analyzed the vehicle gap acceptance behaviors against pedestrians and further proposed an integrated model. The integrated model represented the variations in the maneuvers of left-turners (left-hand traffic) at signalized intersections, and the proposed model dynamically considered the vehicle reaction to intersection geometry and crossing pedestrians [21]. Those research studies focused on analyzing how contextual information affects the driver's behavior.

Recently, researchers applied motion models to control vehicles. Kye et al. presented intention-aware automated driving at unsignalized intersections. The intention-aware decision-making problem is modeled as a partially observable Markov decision process [22]. As for collision avoidance, Kohler et al. proposed to recognize the pedestrians standing at the curb and intending to cross the street despite an approaching car. The proposed active pedestrian protection system can perform an autonomous lane-keeping evasive maneuver in urban traffic scenarios to avoid braking [23]. Keller et al. and Braeuchle et al. proposed an active pedestrian safety system that combines sensing, situation analysis, decision making, and vehicle control. The proposed system can decide whether it will perform automatic braking or evasive steering and reliably execute this maneuver at relatively high vehicle speed [24]. Moreover, Pongsathorn and Akagi et al. proposed to reduce collisions at potentially hazardous areas by suggesting an appropriate speed, which is learned from actual driving data of expert drivers [25,26].

This paper focuses on the scenario at an intersection, one of the most challenging traffic scenarios, and proposes a human-like motion planning model for left-turning vehicles. Fig. 1 illustrates a traffic scenario wherein a vehicle turns and passes an intersection while there are pedestrians walking on or to the crosswalk. In this case, the driver will wait for an appropriate moment and then cross the intersection while iteratively assessing pedestrian situations, making decisions, and adjusting actions. The proposed model represents the whole driving process, as shown in Fig. 2. The proposed model consists of three submodels:

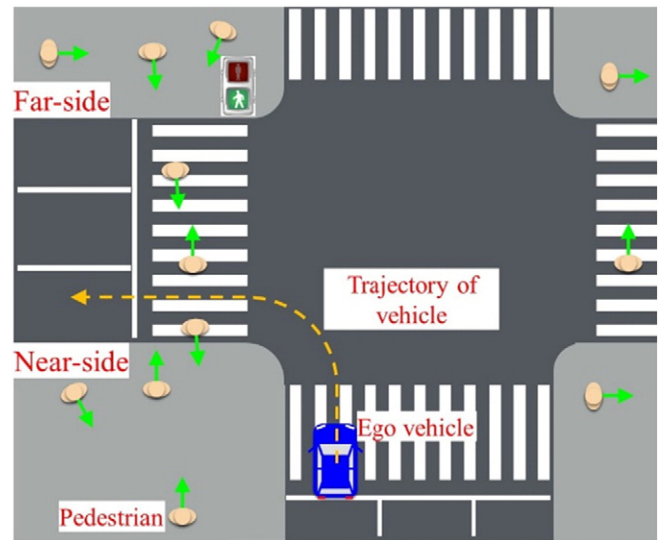


Fig. 1. A left-turning vehicle at an intersection with pedestrians.

pedestrian intention detection model, gap detection model, and vehicle control model. These three submodels are separately responsible for situation assessment, decision making, and action. They also depend on each other in the proposed motion planning model.

In addition, the construction of the motion planning model was conducted on the basis of the analysis of actual human driver data. To obtain a credible model, we collected real data at an intersection in Tokyo City. In the verification of the effectiveness of the proposed idea, the model was implemented as a virtual driver, which allows for comparison with the behavior of human drivers. The contribution of this paper is the development of a human-like motion planning model by integrating a pedestrian intention detection model, gap detection model, and vehicle control model. This paper presents the proposed model and its performance in Sections 2 and 3, respectively. Finally, this paper will be concluded in Section 4.

## 2. Motion planning model

As shown in Fig. 2, the proposed motion planning model includes different submodels. This section explains the construction of each submodel and describes the relationships between the submodels as well. Before the explanations, we clarify the assumptions for the developed models.

- The vehicle trajectory has been determined before the vehicle turns. It means that the proposed model controls the vehicle position along the longitudinal direction rather than changing the trajectory [27]. This assumption is consistent with the common actions of human drivers at intersections.
- The road structure, traffic signal phase, and elapsed time of the phase are assumed to be known, which can be transmitted from a vehicle-to-infrastructure system [28].

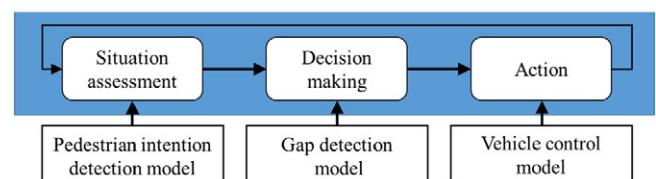


Fig. 2. Flowchart of the proposed motion planning model.

2.1. The pedestrian intention detection model

Pedestrian behaviors are affected by the surrounding traffic situation. The intensive research studies on traffic engineering have suggested that pedestrian behaviors are potentially related to the signal phase, the intersection layout, the vehicles, and even to other pedestrians at signalized intersections [29–31]. Regarding the behavioral flow of pedestrians: assessment, decision making, and physical movement, as a stochastic process, our previous works constructed a probabilistic model of pedestrian behavior using a DBN [32,33]. The developed model takes into account not only pedestrian physical states but also contextual information, and integrates the relationship between them. It is important to note that our pedestrian behavior model can recognize a pedestrian’s crossing or waiting intention before he or she enters the crosswalk area or stops at a road side. The detailed description of the pedestrian behavior model has been published in our previous work [32, 33]. This section describes only the conception of the model.

Fig. 3 illustrates the pedestrian behavior model graphically, which is represented by a DBN. A DBN is a Bayesian network that relates variables to each other over adjacent time steps. Nodes in a DBN, which correspond to the variables in rectangles or ellipses in Fig. 3, represent the temporal process and its possible states. The arcs, which are indicated by solid or dash lines, represent the local or transitional dependencies among variables in a DBN. The construction of a DBN consists of building a network structure and learning the parameters for describing the “arcs.” In this research, parameters in the arcs were learned from actual pedestrian data collected at intersections.

Table 1 summarizes the variables, which are shown in the pedestrian behavior model. As illustrated in Fig. 3, the proposed model first assesses the situation, which is indicated by  $C_t$ . In this research, the contextual information ( $C_t$ ) includes the traffic signal phase ( $Sf_t$ ), the elapsed time of the phase ( $Se_t$ ), the vehicle conditions in the

surrounding environment ( $V_t$ ), the road side relative to the left-turning vehicle ( $Sd_t$ ), the group situation ( $G_t$ ), and the length of the crosswalk ( $Cl$ ). According to the graph, the contextual information ( $C_t$ ), pedestrian positions ( $P_{t-1}$ ), and decision ( $D_{t-1}$ ) at the last time step jointly affect the decision of crossing or waiting at  $D_t$  at the current time step. In fact, the connection between  $P_{t-1}$  and  $D_t$  is represented by  $L_t^d$ , which is the distance to the destination. In the case of a pedestrian preparing to enter a crosswalk ( $W=before$ ),  $L_t^d$  is the distance to the entrance edge of the crosswalk ( $L^{ent}$ ). For a pedestrian in the crosswalk area ( $W=on$ ),  $L_t^d$  is the distance to the exit edge of the crosswalk ( $L^{exit}$ ). This configuration was inspired by actual pedestrian behaviors.

Next, with the contextual information ( $C_t$ ), crossing/waiting decision ( $D_t$ ), pedestrian position ( $P_{t-1}$ ), and motion type ( $M_{t-1}$ ), the model estimates the probability of motion transition, e.g., the possibility that a pedestrian will change from walking to running. The reason we estimate the motion transition is that pedestrians show different distributions of speed at different motion types. After the estimation of  $D_t$  and  $M_t$ , the model predicts the pedestrian speed, moving direction, and pedestrian position. Furthermore, the proposed model uses the observation of the pedestrian position ( $Z_t$ ) to update the probability of the predicted pedestrian position.

To consecutively estimate the pedestrian state including the decision, motion type, and dynamics, we employ a sample-based method, the particle filter (PF) algorithm, as inference. The general PF algorithm has three steps: sampling, importance sampling, and resampling. In the sampling step, which corresponds to the prediction, each particle moves in its state space  $[D_t, M_t, Dr_t, Sp_t, P_t]$  according to its previous state and the proposed graphical model. The probability of the predicted state is evaluated by the contextual information. In the importance sampling step, which corresponds to the correction, the importance weight of each particle is updated on the basis of the observation of the pedestrian position. In the resampling step, particles are reproduced/discarded so

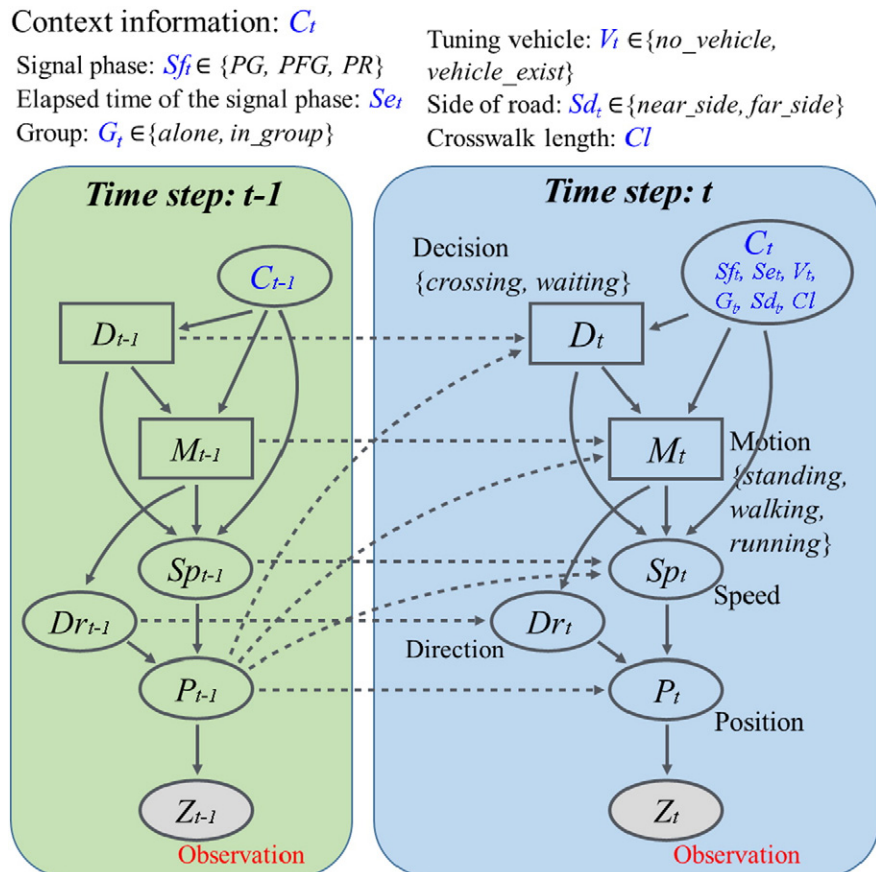


Fig. 3. Proposed DBN model of pedestrian behaviors.

**Table 1**  
Symbols and explanations of the variables used in the proposed pedestrian behavior model.

| Variable | Description   | Notation  |
|----------|---|---|
| $S_f$    | Traffic signal phase for pedestrians                        | $S_f \in \{PG, PFG, PR\}$   |
| $S_e$    | Elapsed time of the current signal phase                    | Unit is seconds   |
| $V$      | Vehicle condition   | $V \in \{no\_vehicle, vehicle\_exist\}$   |
| $G$      | Pedestrian group condition                                  | $G \in \{alone, in\_group\}$  |
| $S_d$    | Crosswalk side  | $S_d \in \{near\_side, far\_side\}$   |
| $Cl$     | Crosswalk length  | Unit is meters  |
| $W$      | Area of the pedestrian's location relative to the crosswalk | $W \in \{before, on\}$  |
| $L^d$    | Distance to the crosswalk entrance/exit                     | $L^d = \begin{cases} L^{ent} & (W = before) \\ L^{exit} & (W = on) \end{cases}$ |
| $D$      | Crossing decision   | $D \in \{cross, wait\}$   |
| $M$      | Motion type of the pedestrian                               | $M \in \{standing, walking, running\}$  |
| $Sp$     | Pedestrian speed  | Unit is meters/second   |
| $Dr$     | Moving direction of the pedestrian                          | Unit is degrees from true north   |
| $P$      | Pedestrian position   | Unit is meters from the original point  |
| $Z$      | Observation of the pedestrian position                      | Unit is meters from the original point  |

that the number of distributed particles will be proportional to the importance weight distribution. Afterwards, all particles are assigned the same importance weights before going to the next epoch. With this mechanism, the pedestrian behavior model can estimate the crossing intention, motion type, moving direction, speed, and position.

2.2. The gap detection model

After obtaining the crossing/waiting intention, position, and speed of pedestrians, the proposed motion planning model estimates which gap is appropriate to pass on the basis of the gap detection model. Generally, a human driver decides whether he or she can pass a gap between two pedestrians when the first pedestrian enters the conflict area of the vehicle trajectory, which was empirically setup as a 2.5-m width in this research. This value was obtained by analyzing real human-driving data. Fig. 4 shows the statistics result on the real human-driving data. The blue line and red line indicate the distributions of the pedestrian distance to the vehicle trajectory at the moment of the drivers accelerating the vehicles, in the case of hard yield and soft yield, respectively. The negative value along the horizontal axis means that the pedestrian has crossed the vehicle trajectory. From this figure, we can see that 85% of the drivers did not start accelerating until the pedestrian had approached the trajectory of about 2.5 m/1.0 m in the case of a hard yield/soft yield, respectively. Moreover, we can see that, in the hard-yield cases, the drivers could accelerate the vehicles earlier than in the soft-yield cases. Thus, our proposed system determined that the conflict area had a 2.5-meter width, and the proposed gap detection model

estimated the probability of gap acceptance on the basis of the situation at this moment (the first pedestrian just entered the conflict area).

Fig. 5 illustrates the configurations of two pedestrians and a vehicle at this moment. The dash line is the vehicle trajectory, and the blue rectangle is the conflict area. Pedestrian 1 just arrives to the conflict area at time  $t$ . At this moment, the distance from pedestrian 2 to the vehicle trajectory is  $D_{p2,t}$ , and the speed of pedestrian 2 is  $V_{p2,t}$ . In addition, the distance from the vehicle to the conflict point is  $D_{v,t}$  and the vehicle speed is  $V_{v,t}$ . This paper proposes to model the gap acceptance behavior using these four parameters. The probability of gap acceptance  $L(\mathbf{x})$  is formulated as follows:

$$L(\mathbf{x}) = \frac{\exp(\alpha + \beta \mathbf{x})}{1 + \exp(\alpha + \beta \mathbf{x})} \tag{1}$$

$$\mathbf{x} = [D_{p2,t}, V_{p2,t}, D_{v,t}, V_{v,t}] \tag{2}$$

where  $\mathbf{x}$  is a vector of explanatory variables;  $\mathbf{x}$  consists of "pedestrian 2" distance  $D_{p2,t}$  and speed  $V_{p2,t}$ , and vehicle distance  $D_{v,t}$  and speed  $V_{v,t}$ .  $\alpha$  and  $\beta$  are a constant and the coefficient for the explanatory variables, respectively. The values of  $\alpha$  and  $\beta$  are learned from actual human driver data using maximum likelihood estimation. The parameters will be visualized in Section 3.3. This model can be used to decide whether to accept or reject the gap according to the output of Eq. (1).

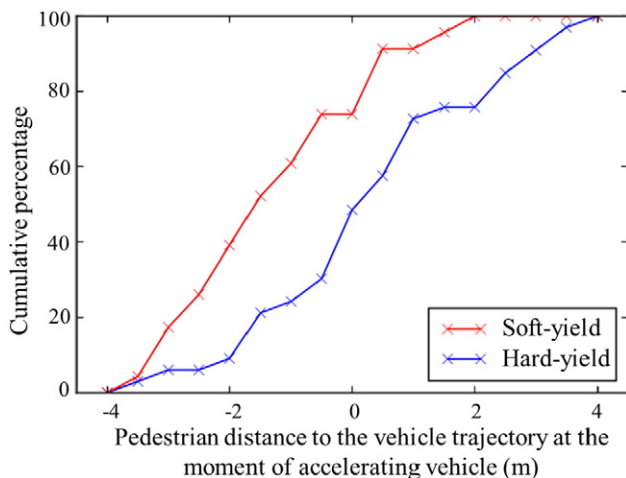


Fig. 4. Distributions of the distance from the pedestrian to the vehicle trajectory.

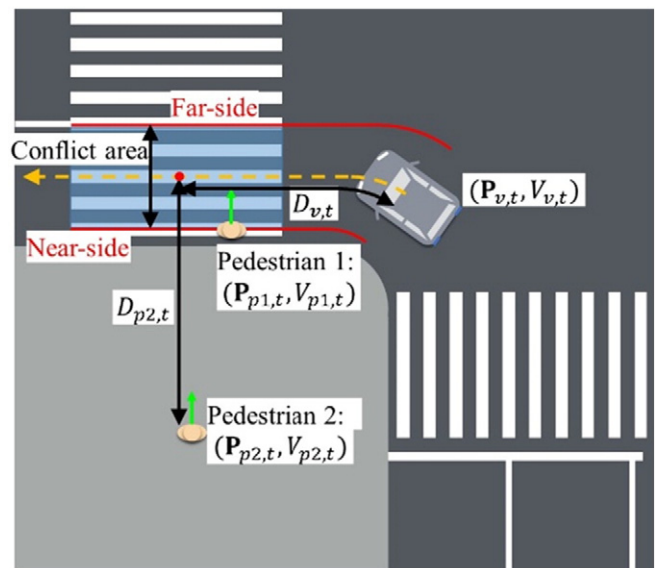


Fig. 5. Illustration of the gap detection model.

Fig. 5 illustrates the case of two pedestrians. In a real traffic situation, this gap evaluation is conducted for all pedestrian pairs. The minimum value of  $L(\mathbf{x})$  among all pedestrian pairs decides whether the vehicle can pass the intersection just after pedestrian 1. The reason we check the minimum value is that we have to consider the worst condition for safety. In addition, our pedestrian behavior model can recognize whether the pedestrian will give up crossing before he or she stops. In the gap detection, we only consider the pedestrians who want to cross the intersection in this signal phase. With the intention recognition, the waiting pedestrians will be excluded in the gap detection.

### 2.3. The vehicle control model

This driving process can be basically divided into the *in-flow* and *out-flow* stages, which correspond to the deceleration before entering a crosswalk and to the acceleration while passing the crosswalk, respectively. Fig. 6 shows the speed of some actual vehicles in the intersection area. The red lines are the speed of the vehicles when there is no pedestrian. In this case, passing an intersection is called *free flow*. The blue and green lines are the speed of the vehicles when pedestrians are present. Obviously, the minimum speed in *free flow* is higher than that in other cases. In addition, some vehicles stop during the period of passing an intersection, such as the blue lines in Fig. 6. This type of passing is called a *hard yield*. In contrast, the green lines do not reach zero during the period of passing. This case is called a *soft yield*. Theoretically, *soft yield* can be considered as a preparation for passing the intersection because the vehicle does not stop and can pass the intersection at a shorter time compared to *hard yield*. This paper proposes to choose either a *hard yield* or a *soft yield* for passing on the basis of the gap detection model.

In most of the cases, vehicles approach an intersection with deceleration and pass it with acceleration. Wolfertmann et al. suggested that the speed curves split according to the acceleration and deceleration, and can be approximated by cubic functions [18]. In this case, the rate of change in acceleration, i.e., jerk, is represented by a linear function. Thus, with the initial jerk  $j_0$ , slope of jerk  $k$ , acceleration  $a_0$ , and speed  $v_0$ , the jerk, acceleration, speed, and distance at time  $t$  can be determined by Eqs. (3) to (6), respectively.

$$j_t = kt + j_0 \quad (3)$$

$$a_t = \frac{k}{2}t^2 + j_0t + a_0 \quad (4)$$

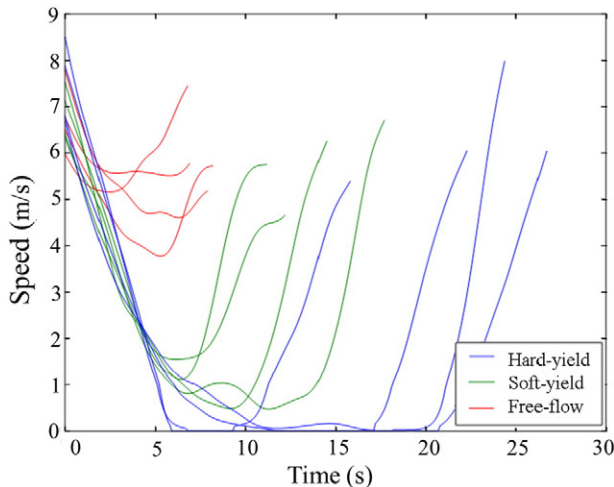


Fig. 6. Vehicle speed at an intersection.

$$v_t = \frac{k}{6}t^3 + \frac{j_0}{2}t^2 + a_0t + v_0 \quad (5)$$

$$d_t = \frac{k}{24}t^4 + \frac{j_0}{6}t^3 + \frac{a_0}{2}t^2 + v_0t + d_0 \quad (6)$$

where the slope of the jerk describes the change rate of the jerk. Generally, a big jerk makes passengers uncomfortable owing to the high dynamics of the inertial force. In this model, if  $j_0$ ,  $k$ ,  $a_0$ , and  $v_0$  are fixed, the speed profile is also determined. It is important to note that our proposed control model does not follow one constant profile. It dynamically chooses the profiles according to the pedestrian conditions. For example, with the expected speed  $v_t$  and acceleration  $a_t$  after  $t$  seconds, the required  $j_0$  and  $k$  can be adjusted using Eqs. (3) to (5).

In a real traffic situation, when there are many pedestrians at an intersection, it is difficult to find a gap to pass the intersection. In this case, drivers usually stop in front of the crosswalks. With the vehicle position, speed, and acceleration at current time  $t$ , the vehicle is expected to stop at the stop point. With this assumption,  $j_0$  and  $k$  can be determined. Alhajyaseen et al. [20] used this profile (stopping profile in the paper) before accepting a gap. Our paper also adopted this idea for generating a *hard-yield* profile.

However, some drivers adopt a *soft-yield* profile for passing the intersection. This paper proposed to use the gap detection model to find potential gaps and determine which profile (*hard-* or *soft-yield* profile) should be chosen. To apply the gap detection model, we need to predict the pedestrian states and vehicle state, to make the first pedestrian satisfy the requirement in the gap detection model. At the predicted moment, pedestrian 1 should just arrive near the edge of the conflict area, as shown in Fig. 5. The predicted states of pedestrian 2 and the vehicle are used for evaluating the acceptance probability of the potential gap using Eq. (1).

If the potential gap is determined, the system moves to the next function, selecting a *hard* or *soft yield*. Fig. 7 visualizes the idea of the profile selection. Suppose that the positions of pedestrian 1 and pedestrian 2 are  $\mathbf{P}_{p1,t}$  and  $\mathbf{P}_{p2,t}$  at time  $t$  and their speeds are  $V_{p1,t}$  and  $V_{p2,t}$ , respectively. At moment  $t$ , the vehicle position and velocity are assumed as  $\mathbf{P}_{v,t}$  and  $V_{v,t}$ , respectively. Pedestrian 1 needs time  $\widehat{\Delta p1f}$  to arrive to the far side of the conflict area:

$$\widehat{\Delta p1f} = D_{p1-f,t} / |V_{p1,t}| \quad (7)$$

where  $D_{p1-f,t}$  is the distance from pedestrian 1 to the far side of the conflict area. Thus, the state of the vehicle can be predicted on the basis of the following equations:

$$\mathbf{P}_{v,t+\widehat{\Delta p1f}} = \mathbf{P}_{v,t} + \int_t^{t+\widehat{\Delta p1f}} V_v(s)ds \quad (8)$$

$$V_{v,t+\widehat{\Delta p1f}} = V_v(t + \widehat{\Delta p1f}) \quad (9)$$

where the vehicle speed is determined by the speed profile  $V_v(s)$  used at time  $t$ .  $V_v(s)$  is the *hard-yield* profile. The proposed vehicle control model determines the type of profile on the basis of vehicle position  $\mathbf{P}_{v,t+\widehat{\Delta p1f}}$  at moment  $t + \widehat{\Delta p1f}$ . If the vehicle follows the *hard-yield* profile  $V_v(s)$  and can arrive to the stop point before or at time  $t + \widehat{\Delta p1f}$ , the system will choose and follow the *hard-yield* profile  $V_v(s)$ . If the vehicle follows the *hard-yield* profile and arrives to the stop point after time  $t + \widehat{\Delta p1f}$ , the system will change to the *soft-yield* profile to catch the gap. In the generation of the *soft-yield* profile, the deceleration of the vehicle at the stop point is constrained to zero, rather than limiting both the speed and the deceleration to zero in the *hard-yield* profile. In addition, the vehicle still decelerates and moves to the stop point, but with a lower deceleration rate.

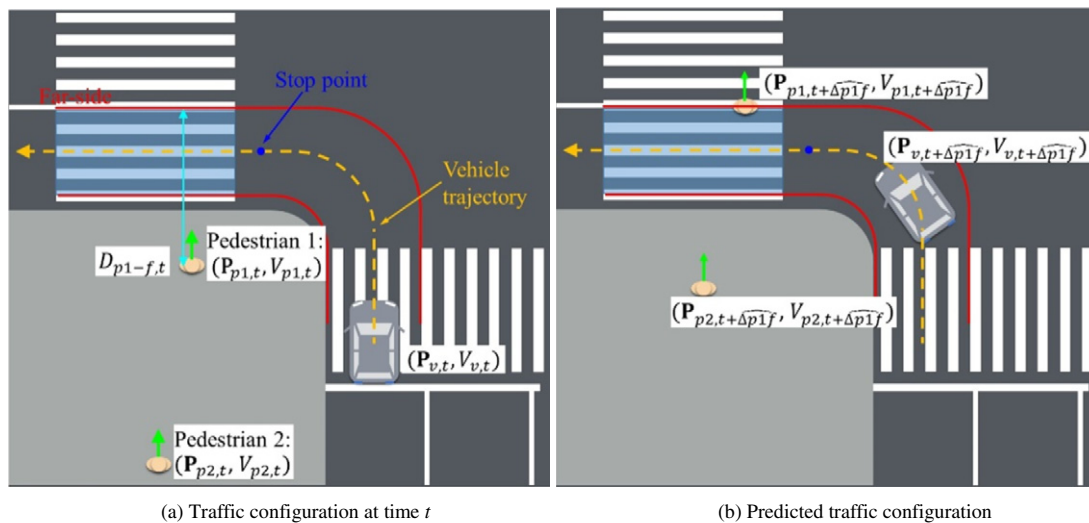


Fig. 7. Illustration of the yield profile selection.

After the vehicle arrives to the stop point, the system evaluates the situation for clearing. In the out-flow profile, the initial jerk  $j_0$  and

slope  $k$  are constant values and empirically determined. Moreover, in the out-flow profile, the system first judges whether the vehicle can

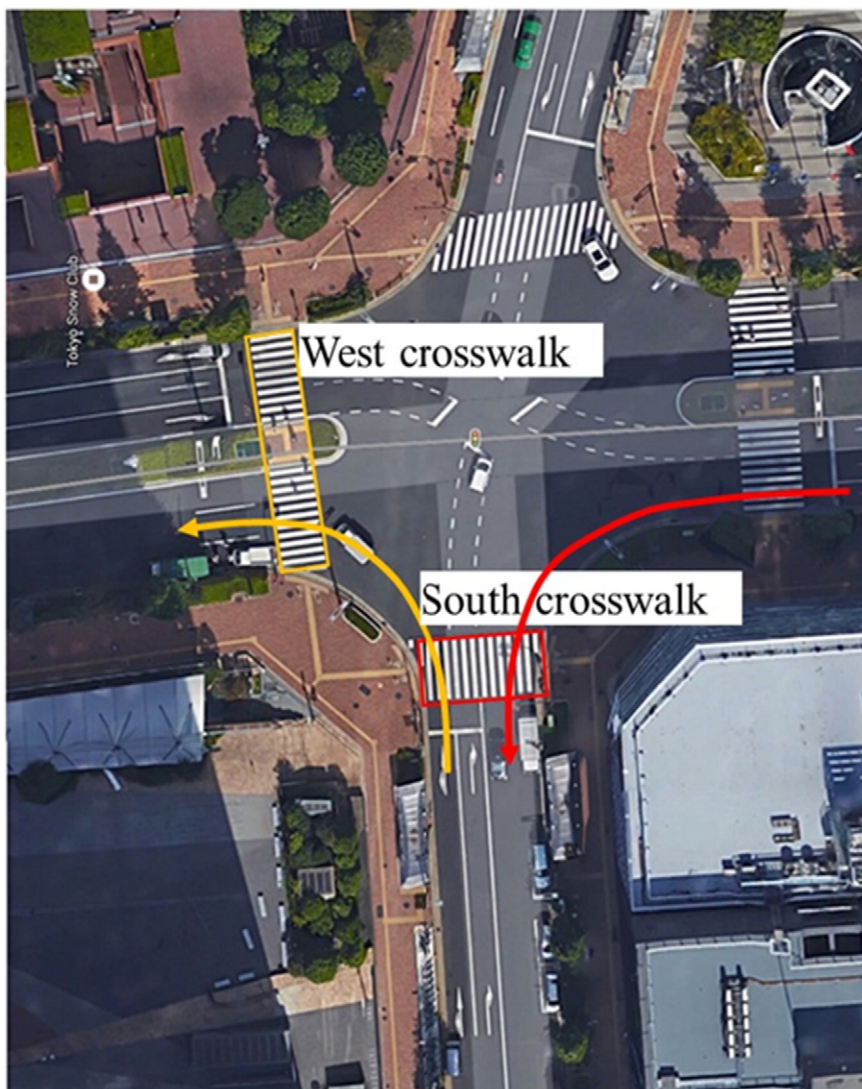


Fig. 8. Road structure of the experiment intersection.



**Fig. 9.** Image captured from a camera installed at a high floor of a building around the intersection. The red points are the labeled pedestrian trajectories, and the green points are the labeled vehicle trajectories.

pass the gap with the determined out-flow profile at every time step. The determination is conducted by maintaining a maximum margin to the pedestrians. If the time is appropriate, the system changes to the out-flow process and passes the crosswalk.

**3. Experiments**

*3.1. Experiment setup and data collection*

To learn and verify the human-like motion planning model, we collected actual data from one intersection in Tokyo City. The road

structure of the intersection is illustrated in Fig. 8, which is a snapshot from Google Earth. We installed cameras at a high floor of a building, which is located around the intersection. Fig. 9 shows the image captured from the camera. The captured video had 10 fps (frame per second) and an 842 × 480 pixel resolution. The captured video was manually calibrated to remove the perspective effect. Because of the occlusion caused by trees and the limited view field of the pedestrian

**Table 2**

Summary of the collected data from the experiment intersection.

|               |           | West crosswalk | South crosswalk | Total |
|---------------|-----------|----------------|-----------------|-------|
| Signal cycles | Total     | 74             | 34              | 108   |
| Pedestrians   | Near side | 374            | 104             | 478   |
|               | Far side  | 339            | 104             | 443   |
|               | Alone     | 533            | 148             | 681   |
|               | Group     | 180            | 60              | 240   |
|               | Crossing  | 614            | 184             | 778   |
| Waiting       | Waiting   | 99             | 24              | 123   |
|               | Total     | 713            | 208             | 921   |
|               | Vehicles  | Left turning   | 117             | 31    |

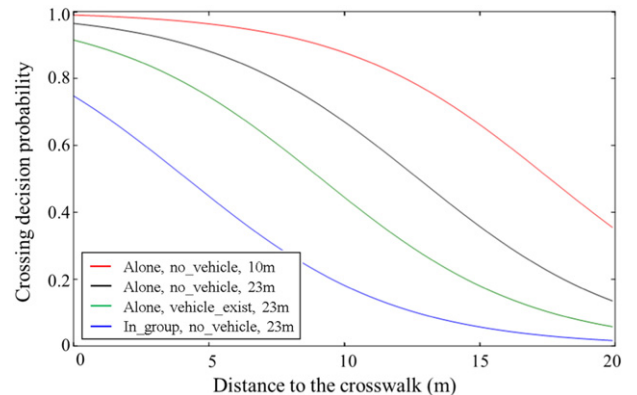


**Fig. 10.** Crossing decision probability at the onset of PFG.

**Table 3**  
Logit regression results of the pedestrian intention recognition model at the onset of PFG.

| Variables                               | Coefficient | Z-value |
|---|-------------|---------|
| Intercept                               | 5.5302      | 5.902   |
| Crosswalk length (m)                    | -0.0968     | -2.601  |
| Pedestrian group condition $\in\{0,1\}$ | -2.2165     | -3.975  |
| Vehicle condition $\in\{0,1\}$          | -0.9314     | -1.887  |
| Distance to crosswalk entrance (m)      | -0.2593     | -5.485  |
| Number of observations                  | 166         |         |
| $R^2$                                   | 0.3321      |         |
| Log-likelihood                          | -71.745     |         |

walking areas, only the “West crosswalk” and “South crosswalk” were considered in this research. The lengths of these crosswalks are 23 m and 10 m, respectively. In this intersection, the cycle time of the traffic signal is fixed. Therefore, we can easily label the signal phase in the whole video by deciding the start time of the first cycle.

The pedestrian and vehicle positions were labeled from the image. An example of the labeling is shown in Fig. 9. The red points and green points correspond to the pedestrians and vehicles, respectively. The sequential position of one vehicle was used as the vehicle trajectory. Because we could not determine the true pedestrian intention at each time step, the decision values were labeled as “waiting” if the pedestrian did not cross. In addition, we applied a Kalman filter to each trajectory and regarded it as the ground truth trajectory. Table 2 shows the statistics of the collected data from the pedestrians and vehicles. Totally, we had 921 pedestrians and 148 left-turning vehicles.

3.2. Evaluation of the pedestrian behavior model

In the evaluation of pedestrian behaviors, we used a fourfold cross-validation to divide the dataset into training and test sequences. The parameters in the proposed model were determined by applying the maximum likelihood estimation in the training sub-datasets. Fig. 10 visualizes the learned relationship between contextual information and crossing probability at the onset of the pedestrian flashing green (PFG) time. Actually, the probability of crossing decision is represented by a logistic function. The variables of the logistic function include the distance from the pedestrian to the crosswalk, vehicle situation, group situation, and crosswalk length. The vertical direction in Fig. 10 is the probability of the crossing decision of pedestrians, and the horizontal direction is the distance from the pedestrian to the edge of the crosswalk. The positive value means that the pedestrian did not enter the area of the crosswalk. It can be seen clearly that the crossing probability, which is the value of the logistic function, increased as the pedestrian was approaching the crosswalk. The different color lines correspond to different contextual conditions. The green line means the crossing probability in the case where a lone pedestrian was crossing a 23-m-length crosswalk with a vehicle waiting. By comparing the green line and the black line, we can see that, if a vehicle appeared at the intersection, the crossing probability would decrease. It means that pedestrians

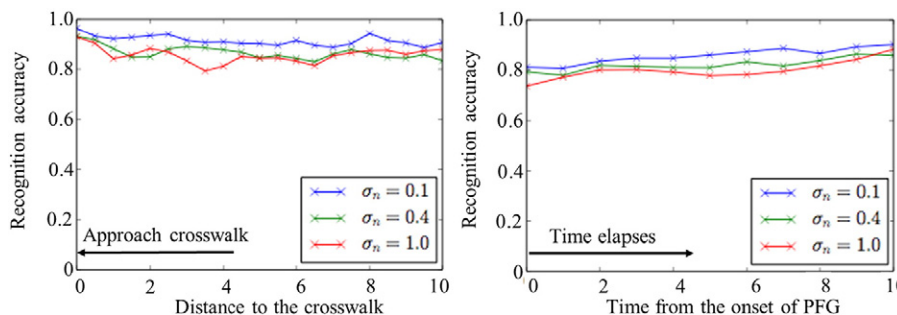


**Fig. 11.** Recognition rate of the crossing/waiting decision with respect to the distance to the crosswalk (left) and to the time from the onset of PDF (right). The different colors indicate the noise level in the position observation.

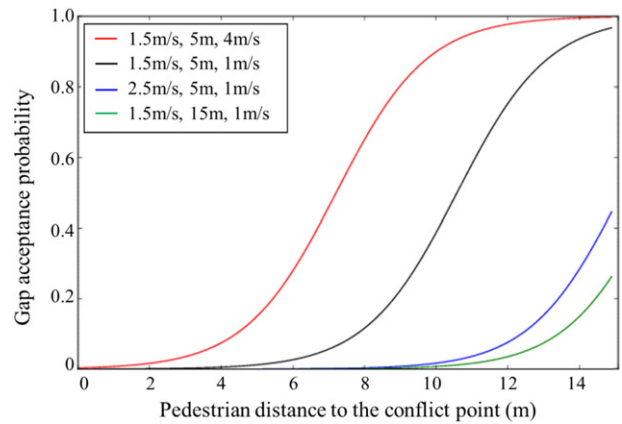


**Fig. 12.** Visualization of the gap acceptance model.

sometimes gave up crossing because of the vehicles. In addition, if the crosswalk was shorter, pedestrians would have more intention to cross during the PFG time, which is indicated by the red line. Moreover, the blue line indicates that pedestrians in group had a lower probability of crossing compared to lone pedestrians (black line).

Table 3 shows the coefficients of the variables obtained from the training. All the four parameters had negative effects on the crossing intention of pedestrians. Moreover, the magnitude of the Z-values indicated the pedestrian group condition and the pedestrian distance to the crosswalk entrance; these two variables are more significant compared to the vehicle condition and the crosswalk length in our model.

In the pedestrian behavior model, the observation was the pedestrian position. We did not directly use the manually labeled position as the observation. The accurate observation could not show the noise tolerance feature of the proposed model. To verify the reliability of the system, we added different levels of the noise to the labeled pedestrian position. The noise was assumed to be normal probability distributions with variances of 0.1, 0.4, and 1.0 m. The DBN model used the noise position as the observation. The decision recognition accuracy is shown in Fig. 11. The left image of Fig. 11 shows the recognition accuracy at different positions relative to the crosswalk. In the smallest position noise case ( $\sigma = 0.1$  m), the proposed model could achieve a 90% recognition rate. In the high-noise conditions, the system still maintained a recognition rate higher than 80%. The right image in Fig. 11 shows the recognition accuracy at different times after the onset of PFG. With the increase in time, the recognition accuracy increased. On average, the system could recognize the pedestrian decision in 83% of the cases at a noise level of 0.4 m.

3.3. Evaluation of the human-like motion planning model

In this paper, we proposed the gap detection model. The probability of the gap acceptance is affected by four parameters: longitudinal



**Table 4**  
Logit regression results of the gap acceptance model.

| Variables                         | Coefficient | Z-value |
|-----------------------------------|-------------|---------|
| Intercept                         | −1.2445     | −1.288  |
| Pedestrian distance (m)           | 0.8220      | 8.593   |
| Pedestrian speed (m/s)            | −3.0379     | −4.623  |
| Vehicle longitudinal distance (m) | −0.4036     | −3.291  |
| Vehicle speed (m/s)               | 1.1051      | 2.897   |
| Number of observations            | 560         |         |
| $R^2$                             | 0.8425      |         |
| Log-likelihood                    | −53.334     |         |

distance from the vehicle to the conflict point, vehicle speed, distance from the pedestrian to the conflict point, and pedestrian speed. The coefficients of the four parameters, which are generated by learning from actual human driver data, indicate how the four parameters affect the probability. Fig. 12 illustrates the relationship between the gap acceptance probability and the parameters. The gap acceptance probability is the value of the logistic function in Eq. (1). The vertical direction in Fig. 12 is the probability of the gap acceptance, and the horizontal direction is the distance from the pedestrian to the conflict point. It can be seen clearly that the probability increased with the increase in distance from the pedestrian to the conflict point. The different color lines correspond to different situations represented by pedestrian speed, vehicle distance, and vehicle speed. The green line means the acceptance probability when a pedestrian was moving at a speed of 1.5 m/s and the vehicle was moving at a speed of 1 m/s at a distance of 15 m. By comparing the green line and the black line, we can see that, if a vehicle moved closer to the conflict point, the acceptance probability would become higher. Moreover, if the vehicle had a faster speed, it would be easy to pass the gaps between pedestrians, which can be concluded by comparing the red line and the black line. It also proves that the soft yield was more effective than the hard yield.

Table 4 shows the coefficients of the variables in the gap acceptance model, which is denoted by Eq. (1). We can see that the pedestrian distance and the vehicle speed were positively affected by the probability of the gap acceptance, whereas the pedestrian speed and the vehicle longitudinal distance had a negative effect on the model. The magnitude of the Z-values indicates that the variables were significant in the gap acceptance model.

Moreover, we evaluated the distance between pedestrians and a vehicle's path when the vehicle arrives to the conflict point. The comparison between human drivers and our proposed model is visualized in Fig. 13. The blue line corresponds to the human drivers, and the red line is estimated from our model. The average difference between two lines was approx. 0.3 m. In addition, the red line is located at the right

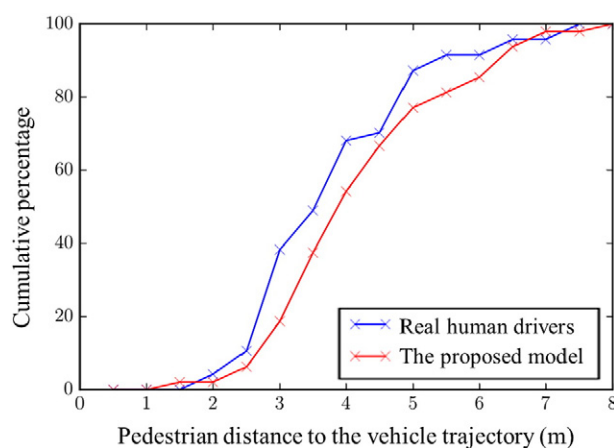


**Fig. 13.** Comparison between real human drivers (blue) and our proposed model (red) for the distance from the pedestrian to the vehicle trajectory at the moment of passing.

**Table 5**  
Similarity in gap acceptance between human drivers and our proposed model/conventional model.

| 48 sequences                      | Same | Delayed | Ahead |
|-----------------------------------|------|---------|-------|
| Proposed model                    | 40   | 7       | 1     |
| Conventional model (3.5-m margin) | 35   | 11      | 2     |

side of the blue line. We can conclude that our proposed model is similar to human drivers and even safer than human drivers. Moreover, the blue line indicates that more than half of the drivers maintained a distance of 3.5 m for a safe margin.

Finally, we compared our proposed model with real human driver behavior to demonstrate how human-like our model is in gap detection. The second row of Table 5 shows the similarity in gap acceptance between our proposed model and human drivers. Our model and human drivers chose the same gap in the 40 cases of 48 total sequences. However, there were 7 cases wherein our model was delayed and 1 case where it was ahead. In fact, the developed model could be considered as equivalent to the average behavior of human drivers. In addition, we also compared our model with a conventional model, which uses a hard-yield profile and fixed comfort margins [34]. The margin was set to 3.5 m, which was suggested by the human driver data in Fig. 13. The third row of Table 5 shows the similarity in gap acceptance for the conventional model. “Ahead” means that the system accepted and passed the previous gaps, which came earlier than the gap selected by the human driver. The result demonstrates that the conventional model had four more delays compared with our proposed method.

One example is shown in Fig. 14, which illustrates the delay case of the conventional model. Fig. 14(a) shows that the vehicle position was controlled by our proposed model, and Fig. 14(b) shows that the vehicle position was determined by the conventional model at the same time as in Fig. 14(a). The black point is the actual vehicle position, which corresponds to the green point in the upper image captured from the camera. We can see that our proposed model entered the crosswalk as the actual driver, but the conventional model stopped outside the crosswalk because it did not accept this gap. There were two reasons for this: The first is that the conventional method only uses a hard-yield profile for in-flow and does not make a preparation for gap acceptance. Our proposed model could maintain a low speed in the in-flow process for quickly passing the smaller gap. The second reason is that our proposed model considers both the pedestrian and the vehicle situations within a logistic function instead of a fixed margin. This mechanism is similar to actual human drivers.

Fig. 15 shows the other case where there was a waiting pedestrian. Pedestrian 2 was the waiting pedestrian. However, this pedestrian was still walking at this moment. Because our pedestrian intention detection model could recognize his or her intention before he or she stopped, the motion planning model could exclude this pedestrian in the gap detection. However, the conventional model had to consider this waiting but walking pedestrian in the gap detection. Therefore, our model started the out-flow process before the pedestrian stopped, which makes the position of our model similar to the actual vehicle, as shown in Fig. 15(a). In contrast, the conventional model had a delay compared to the actual vehicle, which is shown in Fig. 15(b).

#### 4. Conclusions and future work

This paper proposed a human-like motion planning model to represent how human drivers operate vehicles in a signalized intersection. The developed model can assess pedestrians' crossing intention, find the appropriate gap to pass, and optimize the vehicle control profile. The performance of the system was mainly evaluated on the basis of the comparison with actual human pedestrian and driver data. The proposed motion planning model achieved an 83% recognition rate for

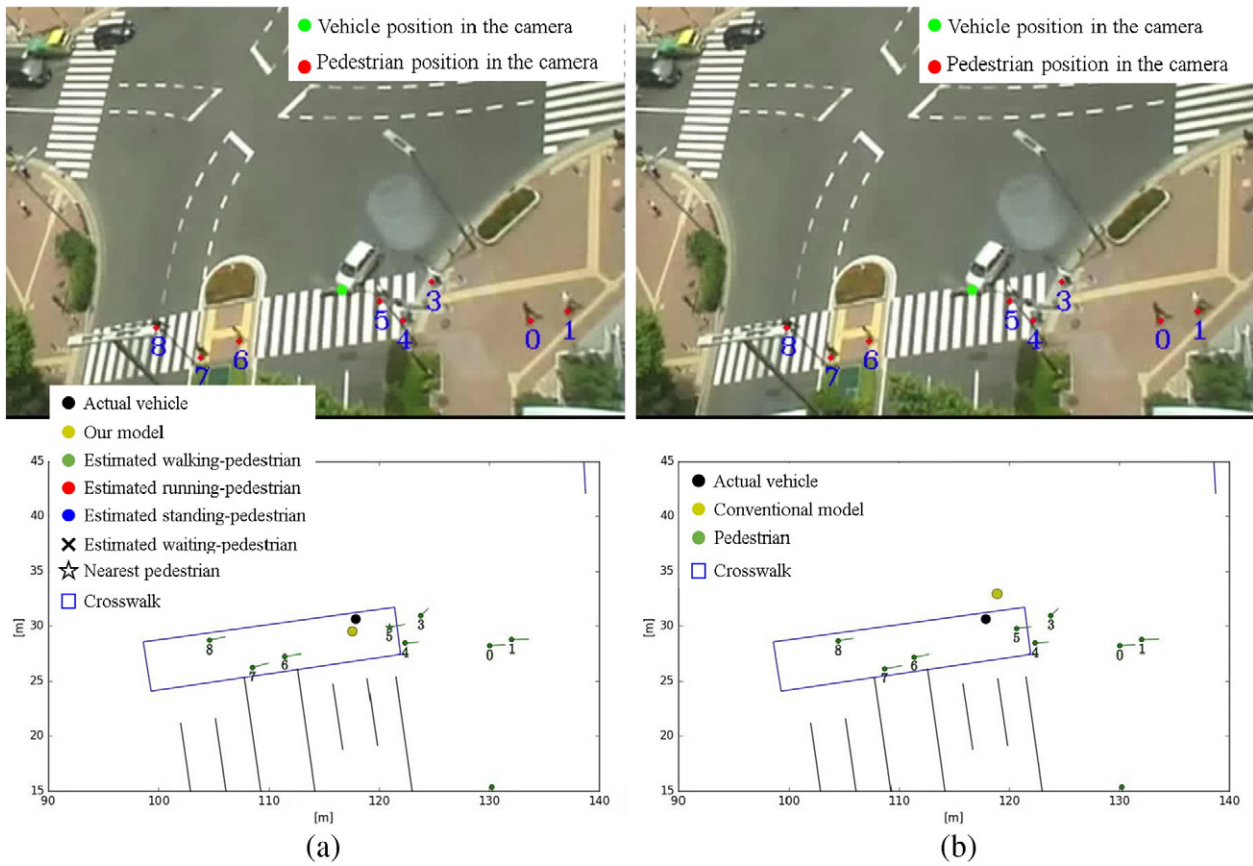


Fig. 14. An example of gap acceptance for the demonstration of the delay case of the conventional model.

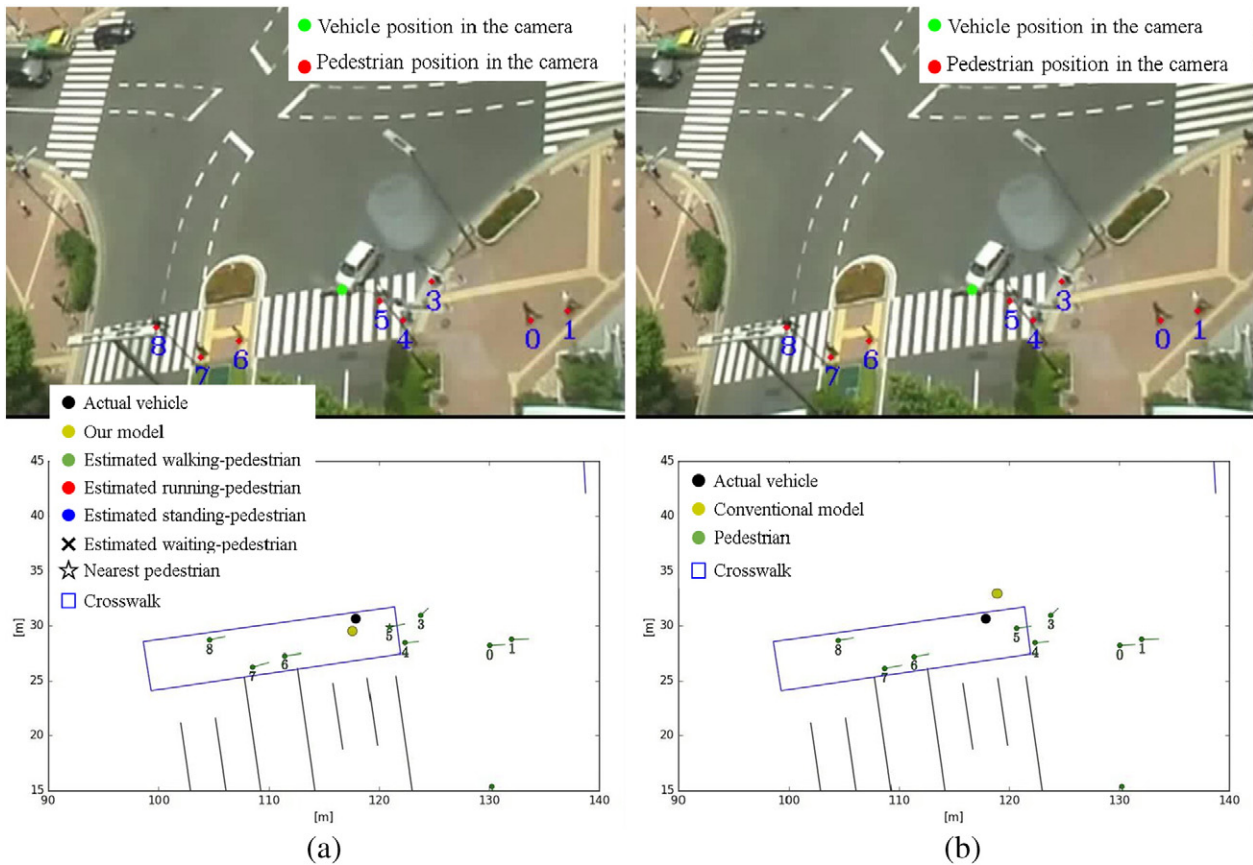


Fig. 15. An example of gap acceptance related to waiting pedestrians.

pedestrian intention. Moreover, the model finally selected the same gap as human drivers did in 83% of the cases.

In this paper, the developed model is represented as a left-turning vehicle as an example because it is one of the most complicated cases in the traffic configuration of Japan. However, the driving behavior in other situations and countries could be explained by the proposed methodology as well. This paper describes the motivation from the viewpoint of autonomous vehicle technology, but the proposed model can also be used for other applications in traffic engineering, such as in the simulation and analysis of the traffic effectiveness of intersections. On the basis of the analysis of the experimental result, we found that a portion of the driver's data were not appropriate as a representative of driving maneuver. The further improvement for our model will be the mining of safe driving maneuver from human driver data. In this way, autonomous vehicles will work just like safe human drivers do. In addition, whether pedestrians recognize the vehicles or not is an important factor for decision making. Combining face detection and decision making would be a good research topic for further works.

### Acknowledgment

This research is permitted by the Compliance Committee of the university.

### References

- [1] Anon. (2015) Driverless Cars Get Into Accidents Because They're Too Good at Driving. <http://mentalfloss.com/uk/technology/34420/driverless-cars-get-into-accidents-because-theyre-too-good-at-driving>.
- [2] S. Lefèvre, D. Vasquez, C. Laugier, A survey on motion prediction and risk assessment for intelligent vehicles, *ROBOMECH J.* 1 (1) (2014) 1–14.
- [3] C.F. Lin, A.G. Ulsoy, D.J. LeBlanc, Vehicle dynamics and external disturbance estimation for vehicle path prediction, *IEEE Trans. Control Syst. Technol.* 8 (3) (2000) 508–518.
- [4] R. Schubert, E. Richter, G. Wanielik, Comparison and evaluation of advanced motion models for vehicle tracking, *Information Fusion*, 2008 IEEE 11th International Conference on 2008, pp. 1–6.
- [5] K. Driggs-Campbell, R. Bajcsy, Identifying modes of intent from driver behaviors in dynamic environments, *Intelligent Transportation Systems (ITSC)*, 2015 IEEE 18th International Conference on 2015, pp. 739–744.
- [6] S.B. Amsalu, A. Homaifar, F. Afghah, S. Ramyar, A. Kurt, Driver behavior modeling near intersections using support vector machines based on statistical feature extraction, *Intelligent Vehicles Symposium (IV)*, 2015 IEEE 2015, pp. 1270–1275.
- [7] T. Gindele, S. Brechtel, R. Dillmann, A probabilistic model for estimating driver behaviors and vehicle trajectories in traffic environments, *Intelligent Transportation Systems (ITSC)*, 2010 13th International IEEE Conference on 2010, pp. 1625–1631.
- [8] T. Gindele, S. Brechtel, R. Dillmann, Learning context sensitive behavior models from observations for predicting traffic situations, *Intelligent Transportation Systems (ITSC)*, 2013 16th International IEEE Conference on 2013, pp. 1764–1771.
- [9] M. Platho, J. Eggert, Deciding what to inspect first: incremental situation assessment based on information gain, *Intelligent Transportation Systems (ITSC)*, 2012 15th International IEEE Conference on 2012, pp. 888–893.
- [10] R. Regele, Using ontology-based traffic models for more efficient decision making of autonomous vehicles, *Autonomic and Autonomous Systems*, 2008. ICAS 2008. Fourth International Conference on 2008, pp. 94–99.
- [11] M. Hülsen, J.M. Zöllner, C. Weiss, Traffic intersection situation description ontology for advanced driver assistance, *Intelligent Vehicles Symposium (IV)*, 2011 IEEE 2011, pp. 993–999.
- [12] Z. Chen, D.C.K. Ngai, N.H.C. Yung, Pedestrian behavior prediction based on motion patterns for vehicle-to-pedestrian collision avoidance, *Intelligent Transportation Systems*, 2008. ITSC 2008. 11th International IEEE Conference on 2008, pp. 316–321.
- [13] D.R. Ragland, S. Arroyo, S.E. Shladover, J.A. Misener, C.Y. Chan, Gap Acceptance for Vehicles Turning Left Across On-coming Traffic: Implications for Intersection Decision Support Design, *Safe Transportation Research & Education Center*, 2006 1–26.
- [14] I.H. Zohdy, Modeling permissive left-turn gap acceptance behavior at signalized intersections, (Master's Degree Thesis), Virginia Polytechnic Institute and State University, 2009 1–117.
- [15] B.J. Schroeder, N.M. Roupail, Event-based modeling of driver yielding behavior at unsignalized crosswalks, *J. Transp. Eng.* 137 (7) (2010) 455–465.
- [16] K. Salamati, B. Schroeder, D. Geruschat, N. Roupail, Event-based modeling of driver yielding behavior to pedestrians at two-lane roundabout approaches, *Transp. Res. Rec.: J. Transp. Res. Board* 2389 (2013) 1–11.
- [17] W.K. Alhajyaseen, M. Asano, H. Nakamura, D.M. Tan, Stochastic approach for modeling the effects of intersection geometry on turning vehicle paths, *Transp. Res. C: Emerg. Technol.* 32 (2013) 179–192.
- [18] A. Wolfermann, W.K. Alhajyaseen, H. Nakamura, Modeling speed profiles of turning vehicles at signalized intersections, In 3rd International Conference on Road Safety and Simulation RSS2011, Transportation Research Board TRB, 2011.
- [19] W.K. Alhajyaseen, M. Asano, H. Nakamura, N. Kang, Gap acceptance models for left-turning vehicles facing pedestrians at signalized crosswalks, *Proceedings of the 3rd International Conference on Road Safety and Simulation*, 2011.
- [20] W.K. Alhajyaseen, M. Asano, H. Nakamura, Left-turn gap acceptance models considering pedestrian movement characteristics, *Accid. Anal. Prev.* 50 (2013) 175–185.
- [21] W.K. Alhajyaseen, M. Asano, H. Nakamura, Estimation of left-turning vehicle maneuvers for the assessment of pedestrian safety at intersections, *IATSS Res.* 36 (1) (2012) 66–74.
- [22] D.K. Kye, S.W. Kim, S.W. Seo, Decision making for automated driving at unsignalized intersection, *Control, Automation and Systems (ICCAS)*, 2015 IEEE 15th International Conference on 2015, pp. 522–525.
- [23] S. Kohler, B. Schreiner, S. Ronalter, K. Doll, U. Brunsmann, K. Zindler, Autonomous evasive maneuvers triggered by infrastructure-based detection of pedestrian intentions, *Intelligent Vehicles Symposium (IV)*, 2013 IEEE 2013, pp. 519–526.
- [24] C.G. Keller, T. Dang, H. Fritz, A. Joos, C. Rabe, D.M. Gavrila, Active pedestrian safety by automatic braking and evasive steering, *IEEE Trans. Intell. Transp. Syst.* 12 (4) (2011) 1292–1304.
- [25] P. Raksincharoensak, Y. Akamatsu, K. Moro, Driver speed control modeling for predictive braking assistance system based on risk potential in intersections, *J. Rob. Mechatronics* 26 (5) (2014) 628–637.
- [26] Y. Akagi, P. Raksincharoensak, Stochastic driver speed control behavior modeling in urban intersections using risk potential-based motion planning framework, *Intelligent Vehicles Symposium (IV)*, 2015 IEEE 2015, pp. 368–373.
- [27] L.D. Adarns, P. Place, Review of the Literature on Obstacle Avoidance Maneuvers: Braking Versus Steering, The University of Michigan Transportation Research Institute, 1994 (Report No. UMTRI-94-19).
- [28] H. Rakha, R.K. Kamalanathsharma, Eco-driving at signalized intersections using V2I communication, *Intelligent Transportation Systems (ITSC)*, 2011 14th International IEEE Conference on 2011, pp. 341–346.
- [29] M. Iryo-Asano, W.K. Alhajyaseen, H. Nakamura, Analysis and modeling of pedestrian crossing behavior during the pedestrian flashing green interval, *IEEE Trans. Intell. Transp. Syst.* 16 (2) (2015) 958–969.
- [30] X. Zhang, P. Chen, H. Nakamura, M. Asano, Modeling pedestrian walking speed at signalized crosswalks considering crosswalk length and signal timing, *Proceeding of the 10th International Conference of the Eastern Asia Society for Transportation Studies*, Taipei, Taiwan, 2013.
- [31] W. Zeng, P. Chen, H. Nakamura, M. Iryo-Asano, Application of social force model to pedestrian behavior analysis at signalized crosswalk, *Transp. Res. C: Emerg. Technol.* 40 (2014) 143–159.
- [32] Y. Hashimoto, G. Yanlei, L.T. Hsu, K. Shunsuke, A probabilistic model for the estimation of pedestrian crossing behavior at signalized intersections, *Intelligent Transportation Systems (ITSC)*, 2015 IEEE 18th International Conference on 2015, pp. 1520–1526.
- [33] Y. Hashimoto, Y. Gu, L.T. Hsu, S. Kamijo, Probability estimation for pedestrian crossing intention at signalized crosswalks, 2015 IEEE International Conference on Vehicular Electronics and Safety (ICVES) 2015, pp. 114–119.
- [34] Kris Hauser, Jeffrey Johnson, Yajia Zhang. (2011) Semiautonomous Longitudinal Collision Avoidance Using a Probabilistic Decision Threshold. IROS Workshop on Perception and Navigation for Autonomous Vehicles in Human Environments, San Francisco, CA, USA,